EFFECT OF TRIANGULAR RIBS ON THE FLOW AND HEAT TRANSFER CHARACTERISTICS OF HEAT EXCHANGER TUBE

by

Shiquan ZHU*, Longjiang LI, Yisen PENG, Chuanxiao CHENG, Wenfeng HU, Zongyao HU, and Tingxiang JIN

School of Energy and Power Engineering, Zhengzhou University of Light Industry, Zhengzhou, China

Original scientific paper
https://doi.org/10.2298/TSCI230130098Z

To improve the heat exchange tube's comprehensive performance and achieve enhanced heat transfer with lower flow resistance. The flow and heat transfer characteristics of a newly enhanced tube with triangular ribs were studied by numerical simulation. The results show that the multi-vortex longitudinal swirl developed in the triangular rib enhanced tube can enhance the cold and hot fluid mixing, and make the temperature distribution in the tube more uniform. The field synergy of velocity and temperature gradient was improved and the heat transfer capacity was enhanced. In the triangular rib enhanced tube, reducing the dimensionless pitch ratio of triangular ribs ($P^* = 0.5$, 0.75, 1, and 1.25) and appropriately increasing the area of triangular ribs ($A = 8$, 12, 16, and 20 mm^2) can improve the performance evaluation criteria (PEC). When $Re = 8475$, $P^* = 0.5$, and $A = 20$ mm^2, the maximum PEC = 1.324 is obtained.

Key words: *heat exchanger tube, heat transfer enhancement, triangular rib, multi-vortex longitudinal swirl*

Introduction

In the endeavor to achieve the goal of sustainable development by 2030, human exploitation of resources should serve the lives of the present generation while providing future generations with sufficient space for development. With the development of society and economy, human consumption of natural resources is increasing, which obliges us to use natural energy efficiently and reasonably, improve the efficiency of energy use and less carbon emission, to limit the human impact on the natural environment. Heat exchanger tubes, as the main equipment for energy exchange, are highly used in chemical, mechanical, electronic, textile, food and pharmaceutical industries, *etc*. [1, 2]. It is significant to augment the heat transfer efficiency of tubes. Recently, researchers have done a lot of work to enhance heat transfer. For the widely used single-phase flow, it is necessary to enhance heat transfer and minimize the flow resistance increase.

Enhanced heat transfer techniques include three categories [3]: active, passive, and composite. Two types of passive techniques are most common, one is the inserted type with coils [4-6], wings/winglets [7-9], and twisted tape [10, 11] that create disturbances for the flow in the tube and promote the mixing of the boundary flow and core flow to achieve enhanced heat transfer. The other type is the shaped tube or the modification of the tube wall. The shaped

* Corresponding author, e-mail: zhusq0701@163.com

tubes include spiral tubes [12], corrugated tubes [13]*, etc.* As for the wall modification, some papers [14] disturbed the boundary-layer by affecting the vortex near the tube wall to obtain more excellent heat transfer performance. Li *et al*. [15] studied a vortex generator with rectangular wings, which formed longitudinal swirls in the tube, and its performance was higher than that of the smooth tube significantly. Habchi *et al*. [16] studied the enhanced heat transfer effect of perforated trapezoidal vortex generators in turbulent flow conditions using numerical simulation, where a pair of vortices in opposite directions existed at the tip of the swirl generator and smaller secondary vortices near the wall, that the perforated structure effectively enhanced the overall performance of the tube. Ding *et al*. [17] studied the heat transfer characteristics of 3-D finned tubes. The heat transfer rate increased rapidly with the increase of fin height, and the highest Nusselt number was obtained for the 3-D finned tube with a fin height is 7 mm, which increased 207% compared to the smooth tube. Li *et al*. [18] studied the internal spiral finned tubes, which changed the flow path of the working fluid, forming a secondary flow, disrupting the temperature boundary-layer, accelerating the heat exchange from the tube wall to the fluid, and enhancing the heat transfer of the tube. Wang *et al*. [19] studied an outward corrugated tube and analyzed the effects of detached swirl and spiral wake. Numerical studies showed that the convective heat transfer on the windward side of the corrugation is transformed into jet impingement heat transfer and causes intense turbulent pulsations in the boundary-layer redevelopment, and the resulting longitudinal swirl suppresses the secondary flow and fluid pulsations. Bhattacharyya *et al*. [20] investigated the thermal characteristics of novel hybrid grooved tape inserts. The heat transfer and flow were analyzed and proved that the novel hybrid grooved tape inserts have a good comprehensive performance. Wei *et al.* [21] investigated sinusoidal wavy tape for enhanced heat transfer, the results revealed that wavy tape can induce the production of secondary flow, enhancing fluid mixing in the near-wall and core-region resulting in more uniform heat transfer in the channel. The passive technique of adding rib on the wall surface of the heat exchanger tube is widely studied, as well as truncated rib [22], *W*-shape rib [23]*, etc.* Moreover, researchers have also proposed some other heat transfer enhancement elements, such as 3-D corrugated circular pipe [24], the micro-fin helically coiled tubes [25], herringbone wavy fin and enhanced fin with convex-strips [26], fin-shaped strips [27]. Zheng e*t al*. [28] proposed discrete inclined ribs. It is found that one rib generates one longitudinal swirl. These swirls mix the fluid between the boundary flow and the core flow, which improves the heat transfer performance. Liang *et al.* [29] proposed finned vortex generators, which induced longitudinal and transverse vortices to improve heat transfer capacity. Lei *et al.* [30] proposed delta-winglet vortex generators, which enhance fluid mixing in the tube resulting in enhanced heat transfer at a relatively small pressure drop.

According to the previous review, longitudinal swirls can be generated either by modification of the tube wall or by inserts in the tube, which can increases the heat transfer capacity. In previous studies [28-30], one pair of spoiler elements can usually produce only one pair of longitudinal swirls. To generate more longitudinal swirls in the heat exchanger tube, we propose a triangular rib spoiler element, and a pair of triangular rib spoiler elements can generate two pairs of longitudinal swirls. In this paper, we use numerical simulation methods to study the effect of triangular ribs on flow and heat transfer, reveal the enhanced heat transfer mechanism of triangular ribs, and analyze the effect of the triangular rib pitch ratio and triangular rib area on flow and heat transfer.

Numerical model

Physical model and boundary conditions

Figure 1 illustrates the 3-D diagram of the fluid calculation domain of the triangular rib tube. The tube wall material is copper. Figure 2 shows the 2-D partial diagram, four triangular ribs are arranged in a set, uniformly arranged around the heat exchanger tube. Tube's inner diameter D_i = 17 mm, tube's outer diameter D_o = 20 mm, inlet section length L_1=100 mm, test section length L_2 = 200 mm, outlet section length L_3 = 100 mm, the dimensionless pitch ratio is the ratio of pitch along the z-axis and tube's outer diameter ($P^* = P/D_o$ = 0.5, 0.75, 1, and 1.25). The triangular ribs are evenly arranged in the test section, and the inlet and test sections are not arranged. The triangle rib is an isosceles right triangle, and the triangle rib area of A = 8 mm^2, 12 mm^2, 16 mm^2, and 20 mm^2 are studied; the triangle rib height t = 0.5 mm.

Assume that the flow is incompressible, 3-D, constant property, steady-state turbulent flow. The working medium in the tube is water, the inlet temperature is 293 K, the inlet velocity is from 0.5-1.3 m/s (the Reynolds number ranges from 8475-22035). the constant and uniform tube wall temperature is 333 K, no-slip boundary conditions for the solid wall; and the outlet is the pressure outlet. The outlet pressure is set to atmospheric (gauge pressure P_{out} = 0 Pa).

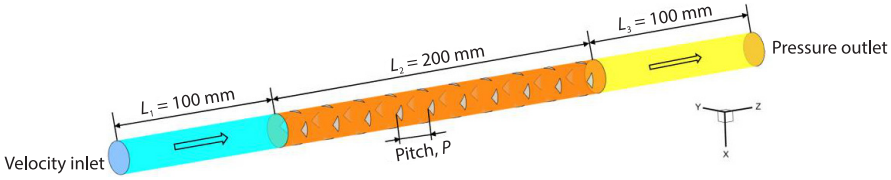

Figure 1. The 3-D diagram of the fluid domain

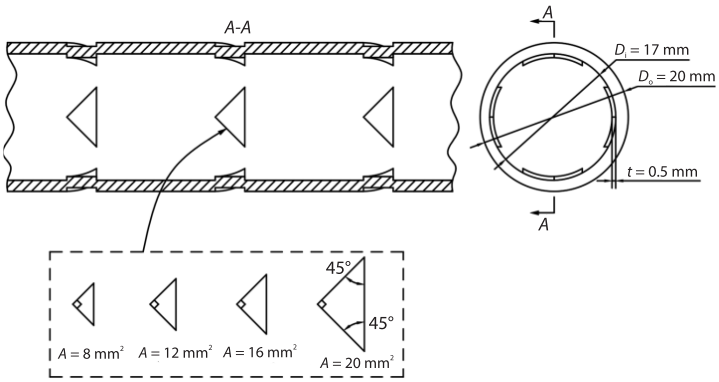

Figure 2. The 2-D partial diagram of the enhanced tube

Parameter definition

The Reynolds number is defined:

$$\mathrm{Re} = \frac{\rho u_m D_i}{\mu} \tag{1}$$

where ρ is the fluid density, u_m – the average velocity, and μ – the dynamic viscosity.

The average heat transfer coefficient, h, is defined:

$$h = \frac{q}{T_w - T_m} \tag{2}$$

where q is the heat flux, T_w – the average temperature of the tube wall, and T_m – the average temperature of the fluid.

The average sselt number in the heat exchanger tube is calculated:

$$\mathrm{Nu} = \frac{hD}{k} \tag{3}$$

where k is the thermal conductivity of water and D – the hydraulic diameter.

The friction coefficient, f, of the fluid in the heat exchanger tube is calculated:

$$f = \frac{\Delta p D_i}{2\rho u_m^2 L_2} \tag{4}$$

where Δp is the pressure drop of the test section, L_2.

To assess the practical use, at the same pump power, defining the performance of flow and heat transfer characteristics of a triangular rib enhanced tube relative to a smooth tube. With Nusselt number and friction coefficient ratios, PEC [31, 32] is defined:

$$\mathrm{PEC} = \frac{\dfrac{\mathrm{Nu}}{\mathrm{Nu}_0}}{\left(\dfrac{f}{f_0}\right)^{1/3}} \tag{5}$$

where Nu_0 and f_0 are the Nusselt number and friction coefficient of the smooth tube, respectively.

Calculation methods and mesh independence test

The turbulence model for solving the control equations is SST k-ω, and the Coupled algorithm is used as a coupled iterative solution for velocity and pressure. When the residuals of the continuity equation is less than 10^{-4}, the other equations are less than 10^{-6}, or the temperature, velocity, and turbulent viscosity ratio of the outlet monitoring are stable and constant, the results can be considered converged.

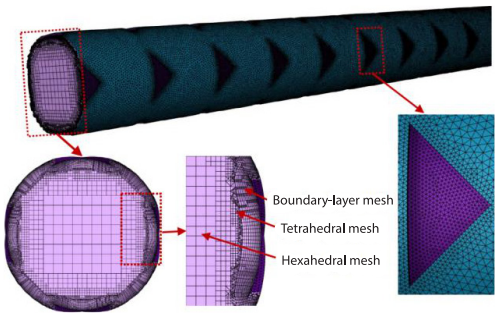

Figure 3. Mesh distribution of the calculation domain

Figure 3 shows the mesh distribution of the calculation domain, the unstructured mesh is generated for the calculation domain using the commercial software FLUENT MESHING. The hexahedral dominance (Hexcore) generation method is used, and sparse hexahedral mesh is used in the central area of the tube. Tetrahedral mesh is used in the contact area with the boundary-layer, the inflation layer mesh Y^+ is less than 1, and the local mesh generated near the ribs was refined.

Figure 4 shows the mesh independence test results. Three different grids with 3.16 million, 5.62 million, and 7.48 million were studied. Compared with 5.62 million and

7.48 million, the difference in Nusselt number was 0.5% and f was 1.9%, so the mesh system of 5.62 million is selected for the study.

Numerical method validation

To evaluate the accuracy of the numerical calculation method in this paper, the numerical calculation results of the smooth tube are compared with the Gnielinski equation and the Petukhov equation [33], shown in eqs. (6) and (7). The maximum deviation of Nusselt number and f is 7.94% and 6.57%, respectively, as shown in fig. 5. Therefore, the numerical simulation results have well matched the empirical correlation equation, which can ensure the accuracy of the numerical simulation.

Gnielinski equation:

$$\mathrm{Nu} = \frac{\frac{\zeta}{8}(\mathrm{Re}-1000)\mathrm{Pr}}{1+12.7\sqrt{\frac{\zeta}{8}}\left(\mathrm{Pr}^{2/3}-1\right)} \tag{6}$$

where $\zeta = (1.821\log\mathrm{Re} - 1.64)^{-2}$.

Petukhov equation:

$$f = \left(0.79\ln\mathrm{Re} - 1.64\right)^{-2} \tag{7}$$

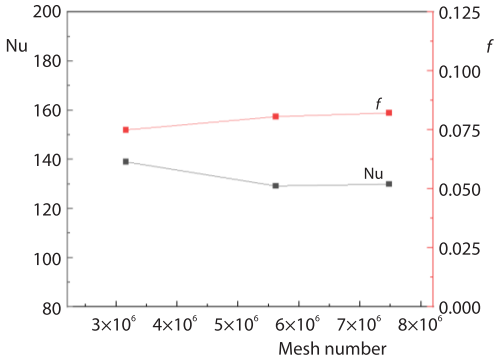

Figure 4. Mesh independence test at $P^* = 0.5$, $A = 16$ mm^2, Re = 8475

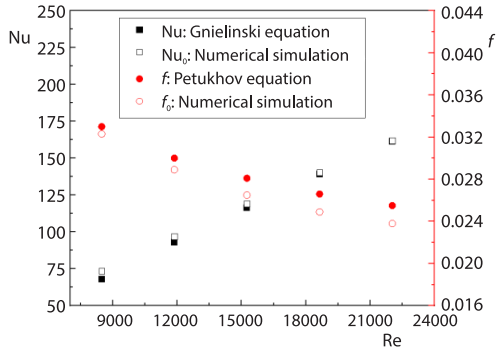

Figure 5. Validation of the smooth tube

Results and discussion

Flow field characteristics

To reveal the heat transfer enhancement mechanism of triangular ribs, the results of the enhanced tube (Re = 11865, $P^* = 0.5$, $A = 16$ mm^2) and smooth tube are compared below. The streamline distributions at four different axial cross-sections are given in fig. 6. The triangular ribs induce the fluid to form four pairs of longitudinal swirls in the heat exchanger tube. The triangular ribs are close to the wall of the high heat tube, and the central area of the fluid is not blocked much, so the resistance does not increase significantly. The longitudinal swirl makes the cold fluid in the center of the tube flow toward the tube wall, which forms damage and scouring to the boundary-layer, promoting the cold and hot fluid mixing, improving the synergy between velocity and temperature gradient, and thus increasing the heat transfer of the tube.

The temperature distributions of the triangular rib enhanced tube (Re = 11865, $P^* = 0.5$, $A = 16$ mm^2) and smooth tube are shown in fig. 7. Under the influence of triangular ribs, the longitudinal swirl strengthens the mixing degree of hot and cold fluids in the boundary and core regions, compresses the boundary-layer thereby obtaining an equivalent thermal boundary-layer with a larger temperature gradient, strengthens the momentum and energy transfer within the boundary bottom layer, and increases the heat transfer capacity significantly. The alternating distribution of cold and hot flows in the enhanced tube promotes the uniformity of fluid temperature distribution inside the tube, resulting in enhanced heat transfer.

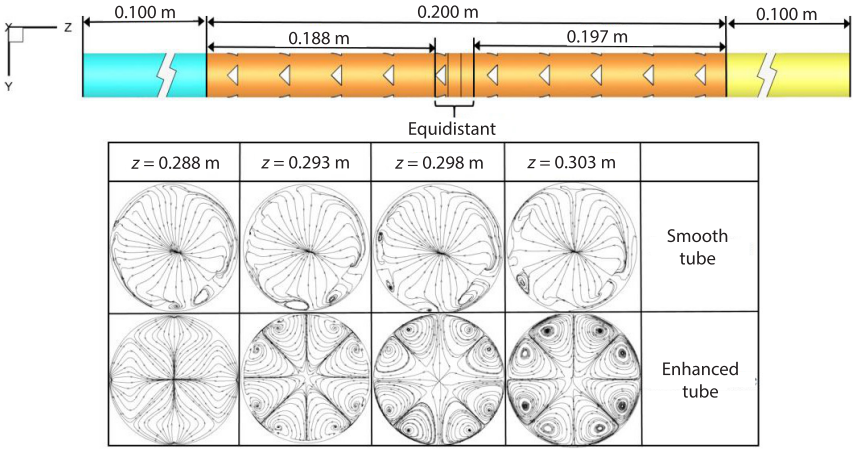

Figure 6. Streamline distribution diagram

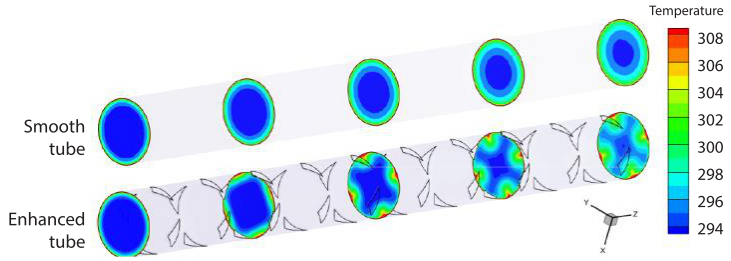

Figure 7. Temperature distributions

The turbulent kinetic energy (TKE) of the triangular rib enhanced tube (Re = 11865, $P^* = 0.5$, $A = 16$ mm^2) and smooth tube are shown in fig. 8. The TKE increases gradually along the axial direction, and the swirl affected region has higher TKE than other regions. This phenomenon can be attributed to the separation and reattachment effect in fluid-flow, which makes the TKE higher in the near-wall area, and the fluid disturbance and mixing drive the mixing of the core flow and boundary flow. The higher the TKE of the fluid, the greater the loss of the mainstream kinetic energy, and the more pump power is required to maintain the flow.

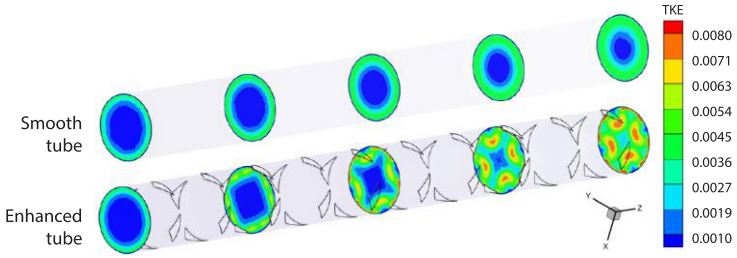

Figure 8. The TKE distributions

The effects of pitch ratio

To explore the effects of pitch ratio on the flow and heat transfer performance of the enhanced tube, the triangular rib area $A = 16$ mm^2 and pitch ratios $P^* = 0.5$, 0.75, 1, and 1.25 were studied. Figures 9(a) and 9(b) illustrates the variation trend of the Nusselt number and

Nu/Nu_0 at different pitch ratios. The heat transfer capacity of the enhanced tube is significantly improved than the smooth tube, indicating that the triangular ribs in the heat exchanger tube can play an essential role in enhancing heat transfer. The Nusselt number and Nu/Nu_0 increase as the Reynolds number increase. As can be seen from fig. 9(a), the smaller the pitch ratio and the larger the Nusselt number for the same Reynolds number, and the increase of Nusselt number is very obvious when the pitch ratio $P^* = 0.5$. As shown in fig. 9(b), Nu/Nu_0 of the enhanced tube is greater than 1 in the range of Reynolds number studied, and the Nusselt number of the enhanced tube is 1.25~1.90 times that of the smooth tube. At the same Reynolds number, the effect of pitch ratio on Nu/Nu_0 is significant, and the enhanced heat transfer performance is better for $P^* = 0.5$ than other pitch ratio cases.

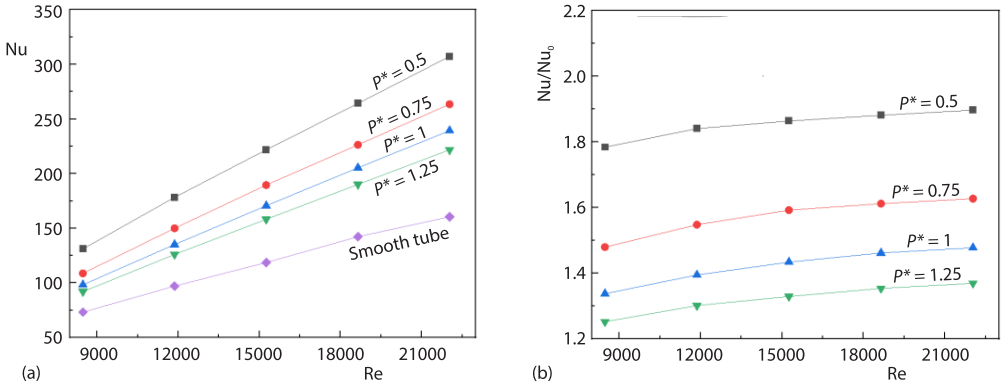

Figure 9. The effects of P^* on heat transfer performance at $A = 16$ mm^2; (a) Nusselt number and (b) Nu/Nu_0

The variation trend of f and f/f_0 with Reynolds number at different pitch ratios is shown in figs. 10(a) and 10(b). The f and f/f_0 of the enhanced tube increase with increasing Reynolds number, and is significantly higher than the smooth tube, f is 1.48~4.19 times that of the smooth tube. The existence of triangular ribs improves heat transfer capacity but also increases the flow resistance, which can be attributed to the additional resistance generated by flow disturbance, separation, and reattachment. Under the same Reynolds number, the f and f/f_0 increase with the decreasing of pitch ratio, and when $P^* = 0.5$, f and f/f_0 increase significantly compared with other cases.

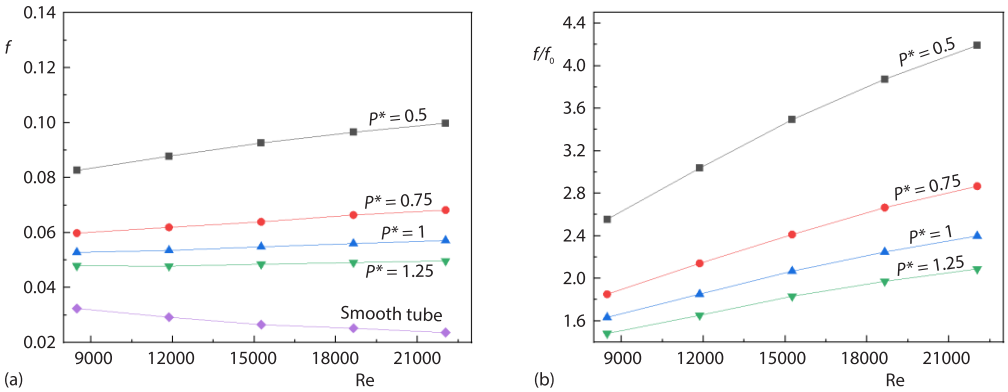

Figure 10. The effects of P^* on flow performance at $A = 16$ mm^2; (a) f and (b) f/f_0

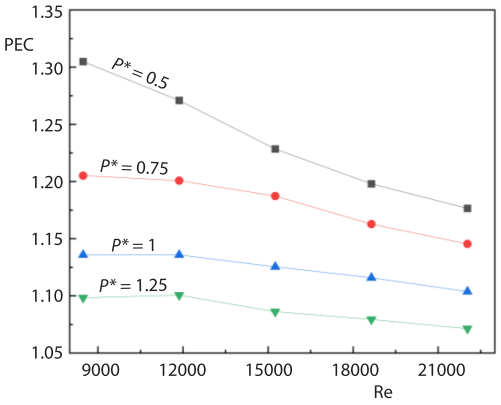

Figure 11. The effects of P^* on PEC (A = 16 mm^2)

The variation trend of PEC with Reynolds number at different pitch ratios is shown in fig. 11. The PEC describes the comprehensive heat transfer index, which is evaluated in heat transfer capacity as gain flow resistance as loss, and the main goal of enhanced heat transfer is to improve heat transfer at a reasonable pressure drop. As fig. 11 shows, the PEC values at different pitch ratios are all greater than 1, which indicates that the triangular rib enhanced tube has a good and obvious enhancement effect. The PEC is better in the lower Reynolds number range, and gradually decreases with increasing Reynolds number. At the same Reynolds number, the PEC increases as the pitch ratio decreases. The maximum PEC value of triangular rib enhanced tube is 1.305.

The effects of the triangular rib area

To investigate the effects of triangular rib area on the flow and heat transfer performance of the enhanced tube, the pitch ratio P^* = 0.5 and triangular rib area A = 8 mm^2, 12 mm^2, 16 mm^2, and 20 mm^2 were investigated. Figures 12(a) and 12(b) illustrates the variation trend of the Nusselt number and Nu/Nu$_0$ at different area. The figure shows that Nusselt number and Nu/Nu$_0$ increase with increasing Reynolds number. Although there is a significant increase in Nusselt number with increasing Reynolds number, the trend of Nu/Nu$_0$ with increasing Reynolds number is relatively gentle. Within the Reynolds number range studied, The Nusselt number of the enhanced tube is 1.59~1.94 times that of the smooth tube. At the same Reynolds number, Nuselt number, and Nu/Nu$_0$ increase with the increase of triangular rib area, but the increase of Nusselt number is relatively insignificant, indicating that the triangular rib area has less effect on Nusselt number.

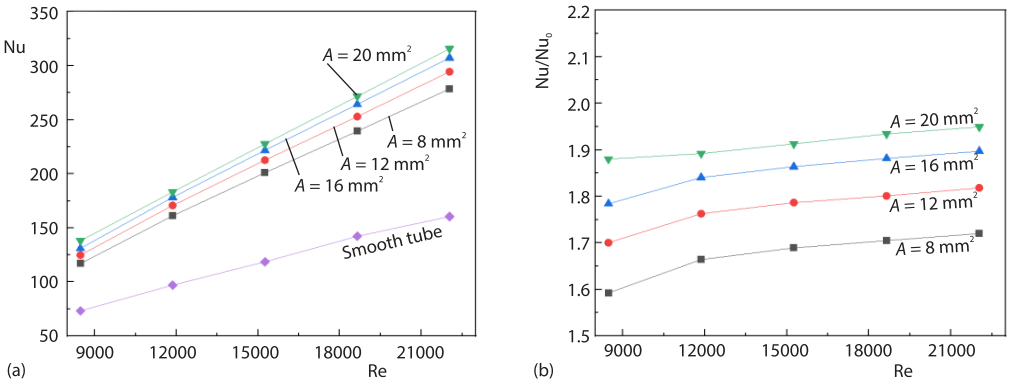

Figure 12. The effects of A on heat transfer performance at P^* = 0.5; (a) Nusselt number and (b) Nu/Nu$_0$

The variation trend of f and f/f_0 with Reynolds number at the different areas is shown in figs. 13(a) and 13(b). The f and f/f_0 of the enhanced tube increase with increasing Reynolds

number, but the increase of Reynolds number has small effect on f and a significant effect on f/f_0. At the same Reynolds number, both f and f/f_0 gradually increase with the increase of the triangular rib area. In the studied range of Reynolds number, f for the enhanced tube is 2.07~4.59 times that of the smooth tube. In fact, the larger the area of the triangular rib, resulting in a larger head-on flow area. The greater the kinetic energy loss of fluid impact on the triangular rib, the more the wall flow is guided by the rib thus changing the initial flow direction, and the greater the resistance generated in the fluid-flow, resulting in the increase of f.

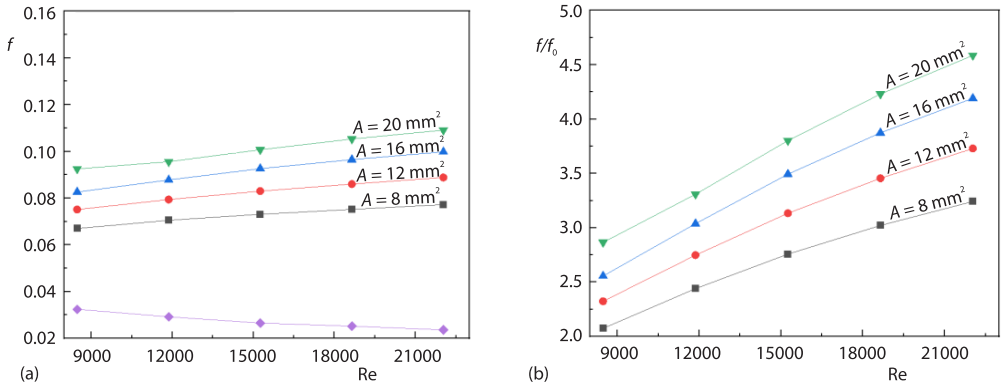

Figure 13. The effects of A on flow performance at $P^* = 0.5$; (a) f and (b) f/f_0

The variation trend of PEC with Reynolds number at the different areas is shown in fig. 14. It can be seen from the figure that the PEC values in all cases are greater than 1, and the maximum value is 1.328, indicating that all four areas of the triangular rib enhanced tube have better comprehensive performance than the smooth tube. Within the Reynolds number range studied, the PEC of the enhanced tube decreases with increasing Reynolds number, and the PEC value has a significantly decreasing trend, and the enhanced tube has better comprehensive performance at the lower Reynolds number. At Re = 8475, the PEC value increases with the increase of the triangular rib area, so increasing the triangular rib area is beneficial to improve the comprehensive performance of the heat exchanger tube. At Re = 11865, in spite of the increase of PEC value with the increase of triangular rib area, the increase of PEC is smaller than that at low Reynolds number, and the increase gradually decreases with the increase of triangular rib area. The PEC value of triangular rib area A = 20 mm² only increased by 0.07% compared with that of A = 16 mm². When Re ≥ 15255, the PEC increases first and then decreases with the increase of the triangular rib area. The difference of PEC values is not significant when the triangle rib area is A = 12 mm², 16 mm², and 20 mm², indicating that the increase in triangle rib area has little effect on the comprehensive performance when $A \geq$ 12 mm² at high Reynolds number.

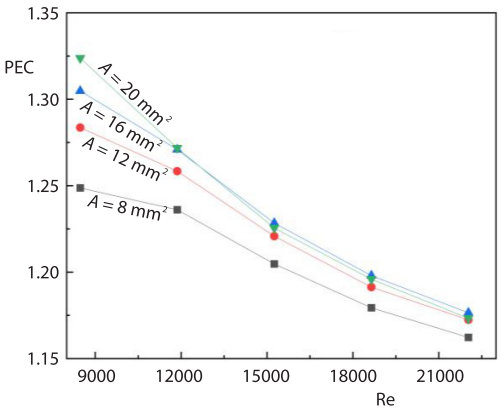

Figure 14. The effects of A on PEC ($P^* = 0.5$)

Conclusions

The heat transfer and flow characteristics of heat exchanger tubes with triangular ribs were studied, and the effect of triangular rib pitch ratio and triangular rib area on the performance of tubes were investigated, compared and analyzed with the calculated results of smooth tubes. The conclusions are as follows.

- The triangular ribs form longitudinal swirls, destroying and scouring the boundary-layer, improving the velocity and temperature gradient synergy, strengthening the mixing of core flow and boundary flow, making the temperature distribution in the tube more uniform, thus enhancing the heat transfer of the tube.
- When the area of triangular ribs A = 16 mm^2, Nu/Nu$_0$, f/f_0, and PEC all increase with the decrease of pitch ratio, and the pitch ratio has an obvious influence on PEC. It shows that the comprehensive performance of the heat exchange tube can be improved by reducing the pitch ratio of the triangular rib.
- When the pitch ratio of triangular rib P^* = 0.5, Nu/Nu$_0$, and f/f_0 increase gently with the increase of triangular rib area. When Re = 8475, PEC increases with the increase of triangular rib area, and the maximum value of PEC is 1.324. When Re ≥ 11865 and A = 12 mm^2, 16 mm^2, and 20 mm^2, PEC values are close to each other and are significantly higher than that when A = 8 mm^2.

Acknowledgment

This work was supported by the Key Scientific Research Projects in Colleges and Universities in Henan Province (21A470007), the Doctoral Scientific Research Foundation of Zhengzhou University of Light Industry (2018BSJJ048).

Nomenclature

A – triangle rib area, [mm^2]
D – hydraulic diameter, [mm]
f – friction coefficient
f/f_0 – friction factor ratio
h – heat transfer coefficient
k – thermal conductivity, [Wm^{-1}K^{-1}]
L – section length
Nu – Nusselt number
Nu/Nu$_0$ – Nusselt number ratio
P – rib pitch, [mm]
P^* – non-dimensional pitch ratio ($P^* = P/D_o$)
Pr – Prandtl number
P_{out} – outlet pressure, [Pa]
Δp – pressure drop of the test section, [Pa]
q – heat flux, [Wm^{-2}]
Re – Reynolds number
T – temperature, [K]
t – triangle rib height, [mm]
u_m – average velocity, [ms^{-1}]

Greek symbols

μ – dynamic viscosity, [kgm^{-1}s^{-1}]
ρ – fluid density, [kgm^{-3}]

Subscripts

1, 2, 3 – inlet section, test section, outlets section
i – inlet
m – mean
o – outlet
w – wall

Acronyms

PEC – performance evaluation criteria
TKE – turbulent kinetic energy

References

[1] Aydin, A., *et al*., Optimization and CFD Analysis of a Shell-and-Tube Heat Exchanger with Multi Segmental Baffle, *Thermal Science*, *26* (2022), 1A, pp. 1-12
[2] Zheng, Z., *et al*., Numerical Study on Transfer and Flow Resistance Characteristics of Multi-Head Twisted Spiral Tube, *Thermal Science*, *26* (2022), 2C, pp. 1883-1895
[3] Sheikholeslam, M., *et al.*, Review of Heat Transfer Enhancement Methods: Focus on Passive Methods Using Swirl Flow Devices, *Renewable and Sustainable Energy Review*s, *49* (2015), May, pp. 444-469

[4] Sharifi K., *et al*., A Good Contribution of Computational Fluid Dynamics (CFD) and GA-ANN Methods to Find the Best Type of Helical Wire Inserted Tube in Heat Exchangers, *International Journal of Thermal Sciences*, *148* (2020), 106398
[5] Dang, W., *et al*., Convective Heat Transfer Enhancement Mechanisms in Circular Tube Inserted with a Type of Twined Coil, *International Journal of Heat and Mass Transfer*, *169* (2021), 120960
[6] Keklikcioglu, O., *et al*., Experimental Investigation on Heat Transfer Enhancement of a Tube with Coiled-wire Inserts Installed with a Separation From the Tube Wall, *International Communications in Heat and Mass Transfer*, *78* (2016), Sept., pp. 88-94
[7] Promvonge, P., *et al*., Thermo-Hydraulic Performance in Heat Exchanger Tube with V-shaped Winglet Vortex Generator, *Applied Thermal Engineering*, *164* (2020), 114424
[8] Liou, T. M., *et a*l., Thermal-Fluidic Correlations for Turbulent Flow in a Serpentine Heat Exchanger with Novel Wing-Shaped Turbulators, *International Journal of Heat and Mass Transfer*, *160* (2020), 120220
[9] Promvonge, P., *et al*., Heat Transfer Augmentation in Solar Receiver Heat Exchanger with Hole-Punched Wings, *Applied Thermal Engineering*, *155* (2019), Mar., pp. 59-69
[10] Kumar, R., *et al*., Modelling of Triangular Perforated Twisted Tape with V-Cuts in Double Pipe Heat Exchanger, *Materials Today: Proceedings*, *46* (2021), 11, pp. 5389-5395
[11] Farhana, A. A., *et al.*, Energetic and Exergetic Efficiency Analysis of a V-corrugated Solar Air Heater Integrated with Twisted Tape Inserts, *Renewable Energy*, *169* (2021), Jan., pp. 1373-1385
[12] Talib, R. N., *et al*., The Effect of External Helical Ribs Tube on the Heat Transfer and Pressure Drop Performance for Multi-Tube Heat Exchanger, IOP Conference Series, *Materials Science and Engineering*, 518 (2019), 032015
[13] Hong, Y. X., *et al*., Heat Transfer and Flow Behaviors of a Wavy Corrugated Tube Applied, *Thermal Engineering*, *126* (2017), Jul., pp. 151-166
[14] Ajarostaghi, S. S. M., *et al*., A Review of Recent Passive Heat Transfer Enhancement Methods, *Energies*, *15* (2022), Jan., pp. 1-60
[15] Li, Y. C., *et al*., Numerical Analysis on Thermohydraulic Performance of the Tube Inserted with Rectangular Winglet Vortex Generators, *Energies*, *15* (2022), Dec., pp. 1-23
[16] Habchi, C., *et al*., Heat Transfer in Circular Pipe Fitted with Perforated Trapezoidal Vortex Generators, *Heat Transfer Engineering*, *43* (2021), Jul., pp. 1-14
[17] Ding, Y. D., *et al*., Experimental and Numerical Investigation on Natural-convection Heat Transfer Characteristics of Vertical 3-D Externally Finned Tubes, *Energy*, *239* (2022), 122050
[18] Li, Y. C., *et al*., A Thermohydraulic Performance of Internal Spiral Finned Tube Based on the Inner Tube Secondary Flow, *Energies*, *15* (2022), Jan., pp. 1-23
[19] Wang, W., *et a*l., Numerical Investigation of Tube-Side Fully Developed Turbulent Flow and Heat Transfer in Outward Corrugated Tubes, *International Journal of Heat and Mass Transfer*, *116* (2018), Sept., pp. 115-126
[20] Bhattacharyya, S., *et al*., Turbulent Flow Heat Transfer through a Circular Tube with Novel Hybrid Grooved Tape Inserts: Thermohydraulic Analysis and Prediction by Applying Machine Learning Model, Sust*ainability*, *13* (2021), Mar., pp. 1-41
[21] Wei, J., *et al*., Heat Transfer Enhancement by Sinusoidal Wavy Tape Insert in Two-Pass Ribbed Channels, *Thermal Science*, *26* (2022), 6A, pp. 4657-4668
[22] Wang, G., *et a*l., Fluid and Heat Transfer Characteristics of Micro-Channel Heat Sink with Truncated Rib on Sidewall, *International Journal of Heat and Mass Transfer*, *148* (2020), 119142
[23] Li, Y., *et al*., Heat Transfer and Pressure Loss of Turbulent Flow in Channels with Miniature Structured Ribs on One Wall, *International Journal of Heat and Mass Transfer*, *131* (2019), Mar., pp. 584-593
[24] Al-Obaidi, A. R., *et al*., Investigation of Flow Pattern, Thermohydraulic Performance and Heat Transfer Improvement in 3-D Corrugated Circular Pipe under Varying Structure Configuration Parameters with Development Different Correlations, *International Communications in Heat and Mass Transfer*, *126* (2021), 105394
[25] Kumar, P. E., *et a*l., Numerical Investigation of Heat Transfer and Pressure Drop Characteristics in the Micro-Fin Helically Coiled Tubes, *Applied Thermal Engineering*, *182* (2021), 116093
[26] Zhang, K., *et al*., Experimental and Numerical Study and Comparison of Performance for Herringbone Wavy Fin and Enhanced Fin with Convex-Strips in Fin-and-Tube Heat Exchanger, *International Journal of Heat and Mass Transfer*, *175* (2021), 121390
[27] Yan, Y. F., *et al*., Numerical Investigation on the Characteristics of Flow and Heat Transfer Enhancement by Micro Pin-Fin Array Heat Sink with Fin-Shaped Strips, *Chemical Engineering and Processing-Process Intensification*, *160* (2021), 108273

[28] Zheng, N. B., *et al*., Numerical Simulation and Sensitivity Analysis of Heat Transfer Enhancement in a Flat Heat Exchanger Tube with Discrete Inclined Ribs, *International Journal of Heat and Mass Transfer*, *112* (2017), May, pp. 509-520
[29] Liang, G., *et al*., Numerical Study of Heat Transfer and Flow Behavior in a Circular Tube Fitted with Varying Arrays of Winglet Vortex Generators, *International Journal of Thermal Sciences*, *134* (2018), Aug., pp. 54-65
[30] Lei, Y. G., *et al.*, Improving the Thermal Hydraulic Performance of a Circular Tube by Using Punched Delta-Winglet Vortex Generators, *International Journal of Heat and Mass Transfer*, *111* (2017), Apr., pp. 299-311
[31] Elsayed, M. L., *et al.*, Thermal design Evaluation of Ribbed/Grooved Tubes: An entropy and Exergy Approach, *International Communications in Heat and Mass Transfer*, *120* (2021), 105048
[32] Dong, Z. M., *et al*., A study On Heat Transfer Enhancement For Solar Air Heaters with Ripple Surface, *Renewable Energy*, *172* (2021), Mar., pp. 477-487
[33] Zhang, K., *et al*., Effects of the Configuration of Winglet Vortex Generators on Turbulent Heat Transfer Enhancement in Circular Tubes, *International Journal of Heat and Mass Transfer*, *157* (2020), 119928

Paper submitted: January 30, 2023
Paper revised: March 13, 2023
Paper accepted: March 15, 2023

© 2024 Society of Thermal Engineers of Serbia
Published by the Vinča Institute of Nuclear Sciences, Belgrade, Serbia.
This is an open access article distributed under the CC BY-NC-ND 4.0 terms and conditions